

2021-2022



MNT and CCDC6 in cutaneous T cell lymphoma cells

Master's Thesis Project

Student: Khoulood Saidi

Institute: Instituto de Biomedicina y Biotecnología de Cantabria (IBBTEC)

Laboratory: Transcriptional control of cancer

Supervisor: Prof. Javier León

I. ABSTRACT

MYC oncoprotein belongs to a protein-interaction network that include proteins of the MXD family, as both MYC and MXD proteins have a common interaction partner: MAX. MYC is deregulated in up to 60% of human tumors and has a crucial role in the initiation and progression of cancer. Unfortunately, MYC has proven to be a difficult therapeutic target. For this reason, the study of the MYC network proteins is important. The most relevant MXD proteins is MNT, because it is ubiquitously expressed and is deregulated in tumors. MNT is labelled as tumor suppressor being an antagonist of MYC, but in some models it cooperates with MYC promoting cell proliferation and survival. Our lab has previously demonstrated a MNT-CCDC6 interaction. CCDC6 is a protein involved in DNA damage repair and a tumor suppressor. Thus, I have studied the activity of MNT and CCDC6 as they can provide the basis for alternative strategies to impair MYC activity in cancer. One of the tumors showing frequent MNT deregulation or deletions is cutaneous T cell lymphoma (CTCL) and thus we focused in CTCL cell lines. First, using Western Blot, I have compared MNT and CCDC6 expression in several human lymphoma cells. Then I have performed co-immunoprecipitation experiments to investigate the MNT-CCDC6 interaction in the cell lines with significant expression of both genes. I have also silenced MNT with short-hairpin methodology, using lentiviral vectors to analyze the effect of MNT depletion on proliferation of the lymphoma cells. Silencing was confirmed by western blot. An increase of proliferation was detected in at least once cell line.

1	INTRODUCTION	1
1.1	MYC-MAX-MXD NETWORK.....	1
1.2	MNT STRUCTURE AND FUNCTIONS.....	3
1.2.1	<i>MNT structure.....</i>	3
1.2.2	<i>MNT regulation</i>	3
1.2.3	<i>MNT alterations in cancer</i>	4
1.2.4	<i>Antagonism and cooperation of MNT with MYC</i>	5
1.2.4.1	MNT as antagonist of MYC	5
1.2.4.2	MNT as cooperator of MYC.....	6
1.2.5	<i>MNT and CCDC6 interaction</i>	6
1.3	CCDC6 STRUCTURE AND BIOLOGY.....	7
1.3.1	<i>CCDC6 isolation</i>	7
1.3.2	<i>CCDC6 structure and function.....</i>	9
1.3.3	<i>CCDC6 role as tumor suppressor gene in cancer</i>	11
1.4	THERAPEUTIC APPROACHES OF CCDC6 IN CANCER	11
2	HYPOTHESIS AND OBJECTIVES.....	12
3	MATERIALS AND METHODS.....	13
3.1	CELL CULTURE	13
3.2	EXTRACTION OF DNA	13
3.2.1	<i>EXTRACTION OF DNA (MNT+CCD6).....</i>	13
3.2.2	<i>PREPARATION OF POSITIVE CONTROLS.....</i>	13
3.3	PROTEIN EXTRACTION AND QUANTIFICATION.....	15
3.3.1	<i>CELL LYSIS, PROTEIN EXTRACTION AND QUANTIFICATION</i>	15
3.3.2	<i>WESTERN BLOT.....</i>	15
3.4	CO-IMMUNOPRECIPITATION	18
3.4.1	<i>PROTEIN LYSATES PREPARATION</i>	18
3.4.2	<i>DYNABEADS IMMUNOPRECIPITATION</i>	18
3.5	LENTIVIRAL INFECTION AND PROLIFERATION ASSAY	19
4	RESULTS	21
4.1	MNT AND CCDC6 EXPRESSION	21
4.2	MNT-CCDC6 INTERACTION.....	22
4.3	EFFECT OF MNT DEPLETION ON CTCL CELL PROLIFERATION	23
5	DISCUSSION.....	25
6	CONCLUSION.....	26

7	FUTURE WORK	26
8	REFERENCES	27

1 INTRODUCTION

1.1 MYC-MAX-MXD network

The proto-oncogene MYC is a basic helix loop helix leucine zipper (bHLHLZ) transcription factor and it is the oncogene most frequently deregulated in human cancer (Kalkat et al., 2017). On the one hand, MYC forms heterodimers with the protein MAX and binds to specific DNA sequences (E-boxes). This complex reacts on different genes include genes involved in cell cycle control, energetic metabolism and genes participating in intercellular communication. Most MYC target genes are activated by MYC (Cowling & Cole, 2006) but it can also repress some of them (Gartel & Shchors, 2003). In addition, MYC can also intensify the transcription activity of genes through a mechanism related with the activation of the p-TEFb (Rahl & Young, 2014). On the other hand, MAX not only interacts with MYC but also with members of the MXD protein family (MXD1, MXI1, MXD3, MXD4 and MNT). This complex, after binding to E-boxes, repress transcription through a mechanism involving histone de-acetylation (Zervos et al., 1993). In consequence, in a particular cell, MYC activity depends on the levels of MXD proteins.

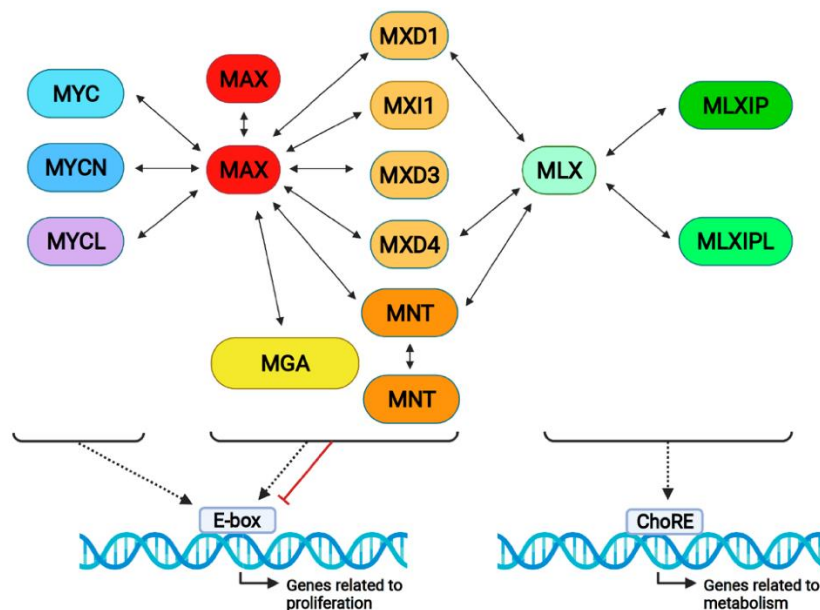


Figure 1.1 MYC-MAX-MNT network. MAX and MNT protein can form homodimers (Liaño pons et al., 2021).

MYC family members is composed of two domains, the transcriptional activation domain (TAD) at the N-terminus, and a bHLHLZ domain bounded to the C-terminus. The TAD is formed of four conserved regions named MYC boxes (MB). First of all, the regulation of MYC protein stability is controlled by MBI due to the phosphorylation of two of its residues, Ser62 and Thr58, by the ERK/MAPK and the PI3K/AKT pathways (Lee et al., 2008). Secondly, MBII mediates the interaction between MYC and distinct coactivators, such as TRAAP, GCN5, TIP60, TIP48, CBP/p300 or SKP2. That is to say, MBII is imperative for MYC transcriptional transactivation function. Moreover, two more MBs have been identified though they are not localized at the TAD region. MBIII which is not only binds to SP1 and/or MIZ-1, and cause a transcriptional repression of MYC, but also interacts with SIN3B leading to the de-acetylation of MYC and its destabilization (Garcia-Sanz et al., 2014). Also, MBIV encloses the nuclear localization signal (NLS) and it is involved in DNA binding and apoptosis (Poole & van Riggelen, 2017). The bHLHLZ domain is necessary for both binding to the DNA (through the basic domain and the helix 1) and interacting with MAX (through the helix 2 and the leucine zipper) (Crouch et al., 1993). MYC structure is schematized in **Figure 1.2**.

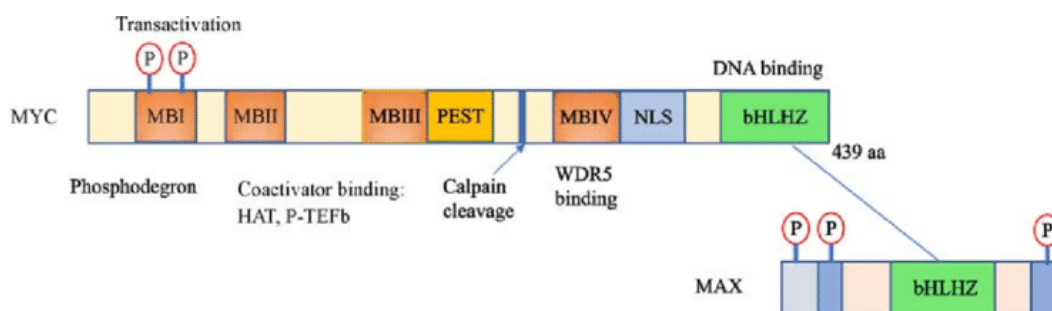


Figure 1.2 MYC gene structure. MYC is composed of 4 conserved boxes MBI-IV, a PEST region rich in proline, glutamic acid, serine and threonine; NLS: nuclear localization sequence; bHLHLZ basic helix-loop-helix leucine zipper domain (adapted from Carroll et al., 2018).

For so long, MYC was known as the oncogene of retroviruses because it was discovered in the retroviruses MC29, CMII, MH2 and OK10. MYC induced, in chicken, a hematopoietic tumor called MYeloCytomatosis. Later, its cellular form located in human chromosome 8q24 was found and due to the huge role of MYC in hematopoiesis, it wasn't surprising that it is heavily involved in lymphoma (Rosenthal & Younes, 2017). MYC would be a therapeutic target as, first, it was shown that after provoking its expression in mice, they developed leukemia or lymphoma (Delgado & León, 2010). As well as, after transient expression of MYC, it was seen sustained lymphoma regression (Gabay et al., 2014). Second, the deregulation of MYC expression, by different known and unknown mechanisms, lead to a variety of aggressive B cells lymphomas, including Burkitt Lymphoma (BL) and Diffuse Large B-Cell Lymphoma (DLBCL) (Xia & Zhang, 2020). As a conclusion, in all these lymphomas, as well as

in lymphoid and myeloid leukemia, MYC activation is associated with high risk of progression and reduced survival (Delgado & León, 2010).

1.2 MNT structure and functions

1.2.1 MNT structure

MNT was discovered in 1997 by two different laboratories that used two distinct methods. The first group found MNT while studying MAX interactions and using cDNA (Hurlin et al., 1997), while the second one identified *MNT* (primitively known as ROX) during working on transcribed sequences of the human chromosome 17p13.3 (Meroni et al., 1997). MNT is a transcription factor composed of two domains: a basic helix-loop-helix-leucine zipper bHLHLZ domain which is specialized in forming dimers with MAX and in binding to DNA on E-boxes, as well as a SIN3 interaction domain which facilitates transcriptional repression (Ayer et al., 1995) (Grzenda et al., 2009). MNT-MAX dimers coexist with MYC-MAX dimers along all phases of the cell. For this reason, MNT plays, not only, a huge role in supervising the oncogenic activities of MYC as being its antagonist or its cooperator, but also a relevant role in cell biology as it is evolutionarily conserved. It is the exclusive MXD protein identified in the fly *Drosophila melanogaster* (Loo et al., 2005). Furthermore, MNT is a fundamental protein for the development as *Mnt* knockout mice die soon after birth (Hurlin et al., 2003a). In addition, *Mnt*-deficient and *Mnt*-overexpressing embryos are of a smaller size and show, respectively, reduced levels of c-MYC and N-MYC (Toyo-oka et al., 2004), and decreased cellularity (Hurlin et al., 1997). In summary, the correct development depends on the control of MNT levels.

1.2.2 MNT regulation

The human *MNT* incorporates six exons according to the NCBI Gene browser (GRCh38/hg38). It encodes a protein with 582-amino acid and four different components. First, at N-terminal region, a coiled-coil α -helix- structure for interaction with SIN3 (SID) which is imperative for the repressive function of MNT. If SID is deleted, MNT protein converts a transcriptional activator (Hurlin et al., 1997). Secondly, a highly proline-rich region involved in protein-protein interactions (Kay et al., 2000) and it is similar to the activation domains of other transcription factors. Thirdly, a BHLHLZ domain necessary for DNA-binding at E-boxes and the interaction with MAX and MLX. Finally, at C-terminal region, a proline and histidine-rich region which ensures the interaction with a member of the NF- κ B family, called REL (Kapoor et al., 2016).

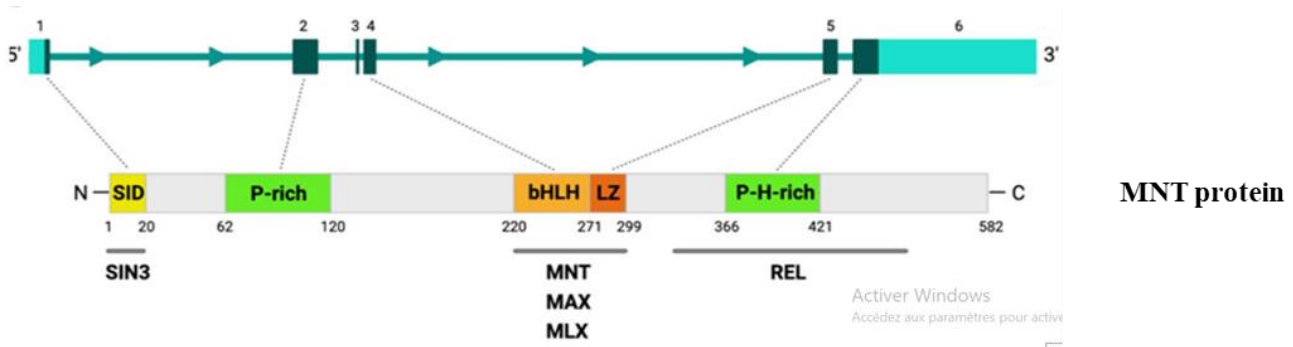


Figure 1.3 MNT human gene, MNT protein and interacting proteins. The MNT gene structure is schematized at the top, with boxes representing the six exons, and a scheme of the MNT protein at the bottom. The MNT exons that encode the most important regions are indicated as boxes, and the dotted lines connect the exons with the corresponding protein domains. The main MNT-interacting proteins are shown at the bottom. SID: SIN3 interacting domain; P-rich: proline-rich sequence; bHLH: basic helix–loop–helix; LZ: leucine zipper; P-H-rich: proline and histidine-rich region; DCD: dimerization and cytoplasmic localization domain (adapted from Liaño pons et al., 2021).

1.2.3 MNT alterations in cancer

MNT is not only an important oncogene in different tumors but also can be a tumor suppressor gene. Its role depends on the several cellular functions in which it is involved, including differentiation, apoptosis, DNA damage, cell cycle, embryonic development, immune system development, inflammation, and NF- κ B pathway regulation (**Figure 1.4**). First, it was discovered that the tissue-specific loss of *Mnt* in mouse models results in thymic lymphoma (Dezfouli et al., 2006) or mammary tumors (Toyo-oka et al., 2006). In addition, MEFs deficient in *Mnt* proliferate faster than wild-type cells and prematurely enter into the S phase (Hurlin et al., 2003b). Finally, in a pan-cancer study of The Cancer Genome Atlas (TCGA) data, heterozygous *MNT* deletion was found in 10% of the tumors (overall frequency) and in more than 20% of liver hepatocellular carcinomas, lung adenocarcinomas, sarcomas, and uterine carcinosarcomas (Schaub et al., 2018).

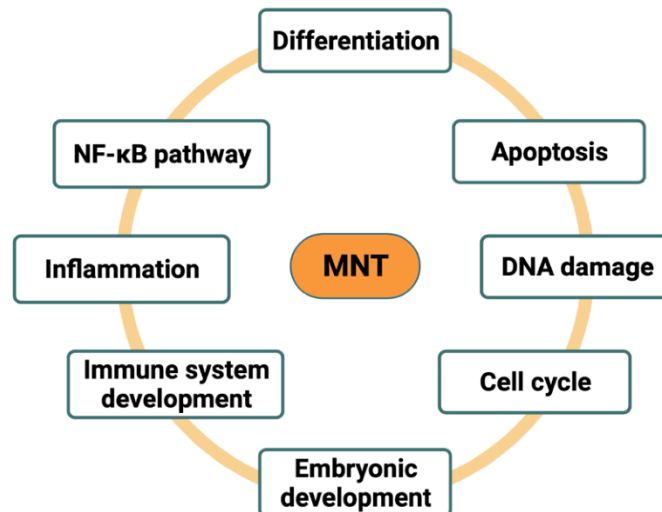


Figure 1.4 The multiple cellular functions of MNT (Liaño pons et al., 2021).

1.2.4 Antagonism and cooperation of MNT with MYC

1.2.4.1 MNT as antagonist of MYC

The expression of MNT is constant throughout the cell cycle, for this reason, MNT-MAX dimers coexist with MYC-MAX dimers along all phases of the cell. This coexistence leads to an antagonism between MNT and MYC. This antagonism is due to a) both MYC and MNT compete for MAX interaction to form an heterodimer (**Figure 1.1**) b) MNT-MAX and MYC-MAX compete for the binding to E-boxes in shared target genes (**Figure 1.1**) and c) MNT-MAX induce the transcriptional repression of genes that are normally activated by MYC-MAX (Orian et al., 2003).

Actually, it has been argued that MYC role is more related to overcoming MNT transcriptional repression than directly due to its transactivation role (Wahlström & Henriksson, 2007). Some studies addressed this statement by using mice and *Drosophila* models. Two studies were done on mice. In the first one, using wild-type mouse embryonic fibroblasts (wt MEFs) versus *Mnt* knockout fibroblasts (*Mnt*^{-/-} MEFs) it was noticed that silencing *Mnt* leads to a faster proliferation with a premature entry to the S phase accompanied by an increase in CDK4 and Cyclin E and a decrease in *Myc* expression. Also, they discovered that *Mnt*^{-/-} MEFs have higher apoptotic rates and have more ability to escape from senescence than wt MEFs. A second study used mice with conditional deletion of *Mnt* in mammary tissue and the results were identical as those observed with *Myc* overexpression as *Mnt* depletion induced adenocarcinomas with a tumor latency of 6-20 months (Hurlin et al., 2003). Indeed, these mammary tumors caused by *Mnt* deletion or *Myc* overexpression have very similar mRNA expression patterns (Toyo-oka et al., 2006).

In addition, two studies were done on cells. To begin with, the experiments were done on quiescent cells where it was observed that *Myc* was well expressed at the G0 to G1 transition while *Mnt* persisted constant as during this transition, there was a switch from *Mnt*-Max to *Myc*-Max dimers (Liaño et al., 2021). Also, this transition led to a switch of MNT-MAX to MYC-MAX dimers. Both *Mnt* overexpression or *Myc* loss arrests cell cycle entry, implying that the ratio of MNT versus MYC levels may determine the quiescent or proliferative state of the cell (Walker et al., 2005). Second, *MNT* deletion in T cells induced a rise of both proliferation and apoptosis. This was accompanied by tumor formation with a long latency, the disruption of T-cell development, and the enlargement of the secondary lymphoid organs (Link & Hurlin, 2015).

Finally, one study was carried out on *Drosophila* and showed the same results as found in mouse models and in humans. Indeed, both genes that were found were *dMNT* and *dMYC* and have opposing activities (Orion et al., 2003). Although there are different causes for MNT-MYC antagonism, it remains partial due to the different bHLH domain sequences and DNA affinities. Furthermore, while MYC can only form a dimer with MAX, MNT can make at least three other different complexes with another MLX protein as MLX (**Figure 1.1**).

1.2.4.2 MNT as cooperator of MYC

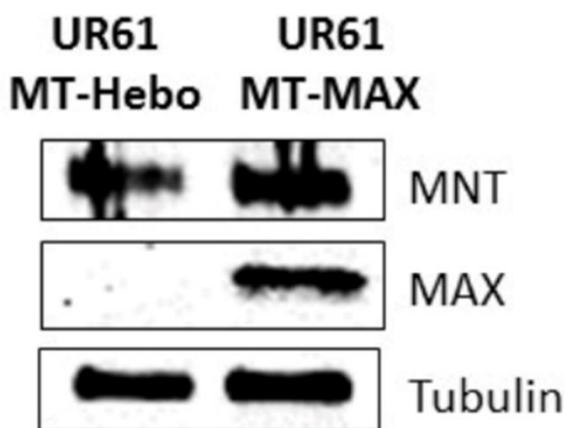
In contrast with the data represented above, it was shown in some reports that, although some of the mechanisms are still not known, *MNT* can also be as a cooperator of *MYC*. This result was first proved in thymocytes as provoking both *Mnt* knockout and *Myc* overexpression, in mice, leads to higher apoptotic levels than each one of them alone (Link et al., 2012). In addition, *Mnt* heterozygosity reduces *Myc*-driven B and T-lymphomagenesis. This result was observed on two *Myc* transgenic models (Campbell et al., 2017) but the mechanism was not defined as the researchers did not notice any changes in populations, cell cycle or apoptosis. Finally, in MYC-driven B lymphomagenesis, the IL-7 receptor controls at the same time *MNT* and *MYC* and *MNT* overcomes apoptosis by repressing Bim which promotes *MYC* activity (Liaño et al., 2021). For this reason, *MNT* anti-apoptotic functions must be key to compensate for increases in MYC levels during lymphopoiesis.

1.2.5 MNT and CCDC6 interaction

CCDC6 is a tumor suppressor and it is an important protein for its important role in the response to DNA damage (discussed below in point 3). In a study from my laboratory aimed to determine MNT-interacting proteins different from MAX, it was discovered an MNT-CCDC6 interaction in UR61 cells (Liaño et al., 2021). In that study, two cell lines of rat pheochromocytoma were used: UR61-MT-Hebo which lack MAX protein and UR61-MT-MAX, a UR61 derivative harboring an expression vector human MAX (**Figure 1.5a**). Proteins from both cell lines were subjected to a proteomic analysis. MNT immunoprecipitation was performed and the immunoprecipitated proteins were analyzed by mass

spectrometry. Comparing the results with both cells, the proteins that bind to MAX could be sorted out and thus aimed to proteins interacting with MNT. The proteomics analysis showed that five proteins were bound to MNT, one of them was CCDC6 protein (**Figure 1.5b**) which proves that CCDC6 interacts with MNT, at least in UR61 cells. But, until nowadays, no more results of this interaction were described in other cell lines, for this reason, in my master's project I am trying to search for this interaction in CTCL cells after proving, by western blot, that they express an important amount of both genes MNT and CCDC6.

a)



b)

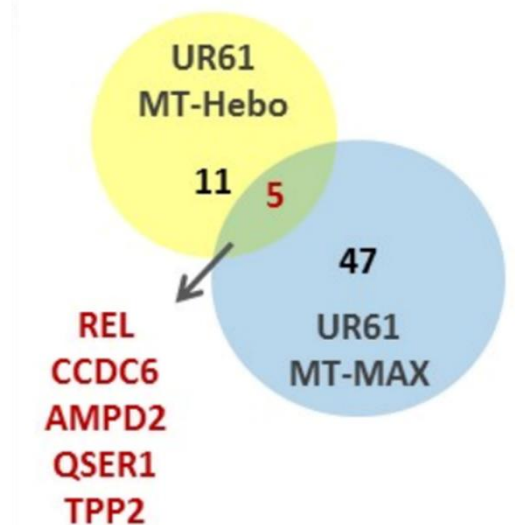


Figure 1.5 MNT interacting proteins. a) Expression of MNT in both UR61 MT-Hebo and UR61-MT-MAX cells but expression of MAX only in UR61-MT-MAX. Tubulin was used as a protein loading control. b) Schematic representation of the positive interactions found in the proteomics assays. REL, CCDC6, AMPD2, QSER1 and TPP2 were found in both UR61 MT-Hebo and UR61-MT-MAX immunoprecipitations.

1.3 CCDC6 structure and biology

1.3.1 CCDC6 isolation

After transfections experiments in NIH3T with DNA from papillary thyroid carcinoma, it was isolated a rearranged gene between the tyrosine kinase receptor RET and a new gene, this was called Coiled Coil Domain Containing 6 gene, known as CCDC6. The rearrangement of CCDC6 protein produces a fusion gene containing the N-terminal region of it and the intracellular kinase-encoding domain of RET protooncogene, which shows a constitutive kinase activity (Jiang, 2000). CCDC6 can also be called PTC for papillary thyroid carcinoma as, in 10-25% of the cases, the fusion of CCDC6

with the gene RET was identified (Grieco et al., 1990). For several years, it was thought that the only partner of CCDC6 was RET until the discovery of many others partners. In addition, each fusion is responsible of a type of tumor not only papillary thyroid carcinoma (Cerrato, Visconti, et al., 2018) (Laxmi et al., 2019) (**Figure 1.6**).

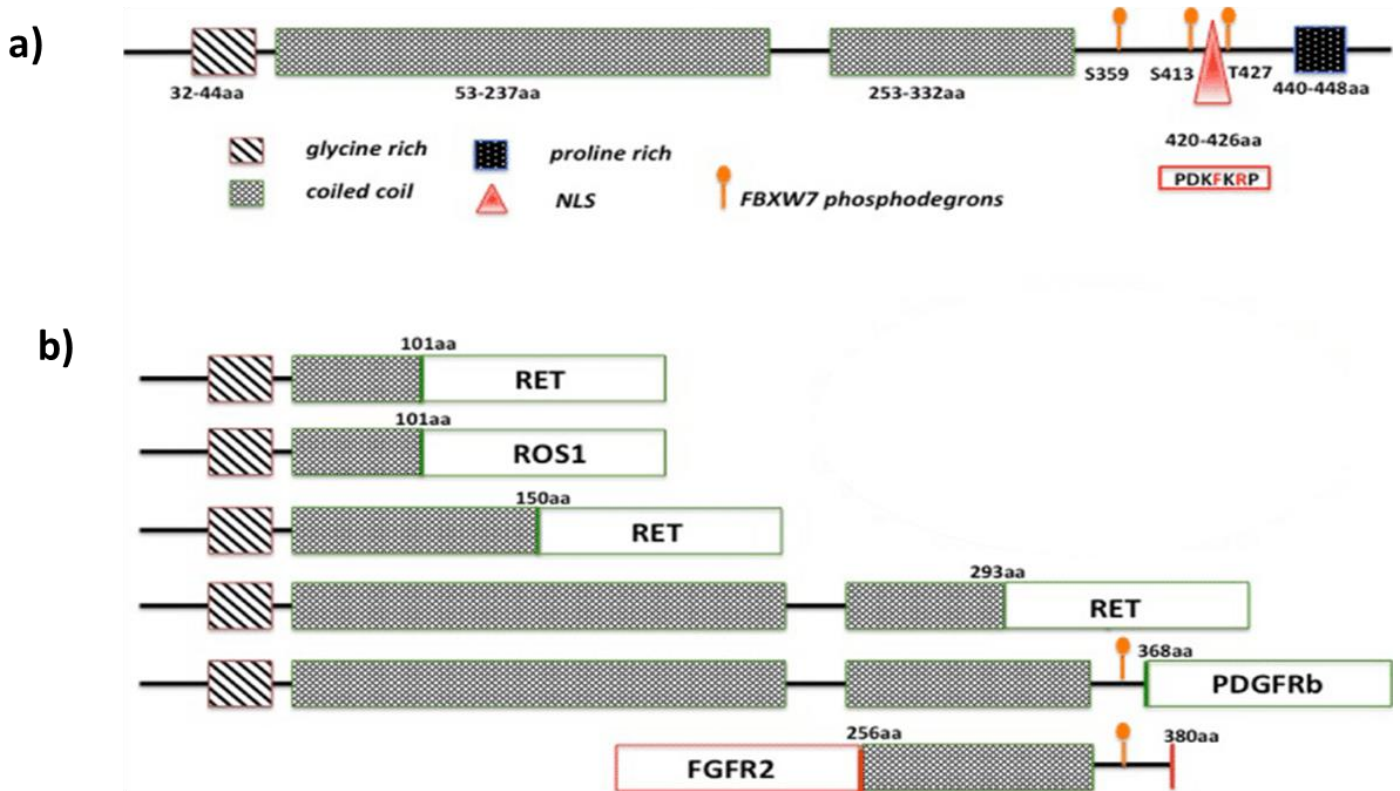


Figure 1.6 structure of CCDC6 protein and its different partners. a) Scheme of the CCDC6 protein showing the relevant domains. b) Scheme of the CCDC6 fusion proteins originated by chromosomal translocations found in cancer. (Cerrato, Merolla, et al., 2018).

There are described at least 10 TCCDC6 translocations partners in cancer (**Table 1**) and it has been found mutated in a small fraction of tumors (**Table 1 and described below**). Moreover, a low expression of CCDC6 has been reported in lung and prostate cancer (**Table 1**).

Table 1: Molecular alterations of CCDC6 found in human cancer (Cerrato, Merolla, et al., 2018)

CCDC6 alteration	Tumor type
CCDC6/RET	<i>Thyroid</i>
CCDC6/PDGFR	<i>NSCLC</i>
CCDC6/PTEN	<i>Colon</i>
CCDC6/ANK3	<i>Leukemia (CML)</i>
CCDC6/UBE2D1	<i>Thyroid</i>
FGFR2/CCDC6	<i>Ovarian epithelial tumor</i>
CCDC6/LIPI	<i>Breast cancer</i>
CCDC6/CTNNA3	<i>Breast cancer; iCCA</i>
CCDC6/ROS1	<i>NSCLC</i>
KITLG/CCDC6	<i>NSCLC</i>
	<i>NSCLC</i>
<i>CCDC6 mut.* 0, 1-1%</i>	<i>Breast, Endometrium, Ovary Large intestine, Liver, Lung Pancreas, Prostate, Thyroid etc.</i>
<i>CCDC6 gene expression</i>	<i>Breast, Endometrium, Cervix Large intestine, Liver, Lung Pancreas, Prostate, Thyroid Stomach etc.</i>
<i>CCDC6 protein levels are reduced in 20% of cases</i>	<i>NSCLC SCLC Prostate</i>

1.3.2 CCDC6 structure and function

CCDC6 is located on chromosome 10 and encodes for 475 amino acids in humans. It contains a lengthy region of alpha helices which is responsible of the coiled coil conformation (**Figure 1.7**). CCDC6 is highly conserved and is ubiquitously expressed in human tissues, in the nucleus and the cytoplasm. In addition, it has been proved that CCDC6 contains coiled coil region that has the ability of protein dimerization and oligomerization which suggested its possible role in protein-protein interactions (Laxmi et al., 2019). CCDC6 has different functions inside the cell. First of all, it can be either phosphorylated by ERK2 upon serum stimulation or by ATM in response to genotoxic stress (**Figure 1.8**) which leads to its stabilization in the nucleus where it can interact with the catalytic subunit of the PP4C phosphatase and inhibits the phosphatase activity on the phosphorylated S139 residue of the histone H2AX (Cerrato, Merolla, et al., 2018) (**Figure 1.8**). In addition, CCDC6 can repress CREB1 which is a DNA nucleotide sequence present in many viral and cellular promoters and is responsible of the transcription (Leone et al., 2010) (**Figure 1.8**).

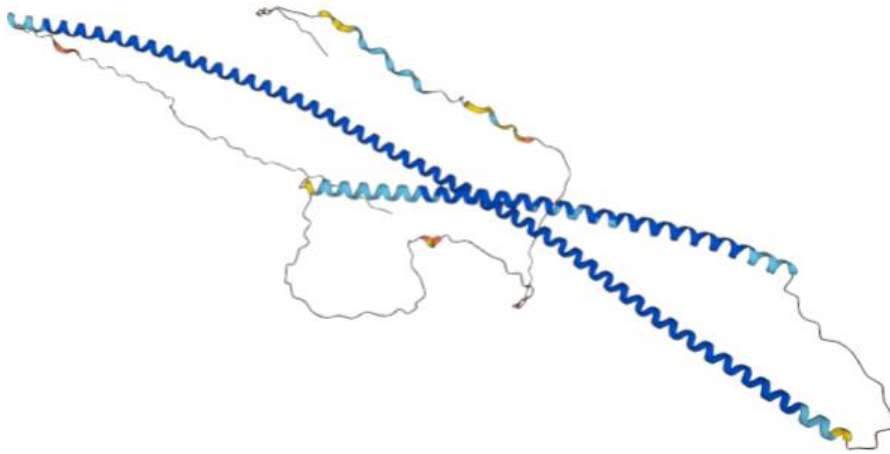


Figure 1.7 The structure of CCDC6 protein predicted by the Alpha-fold software.

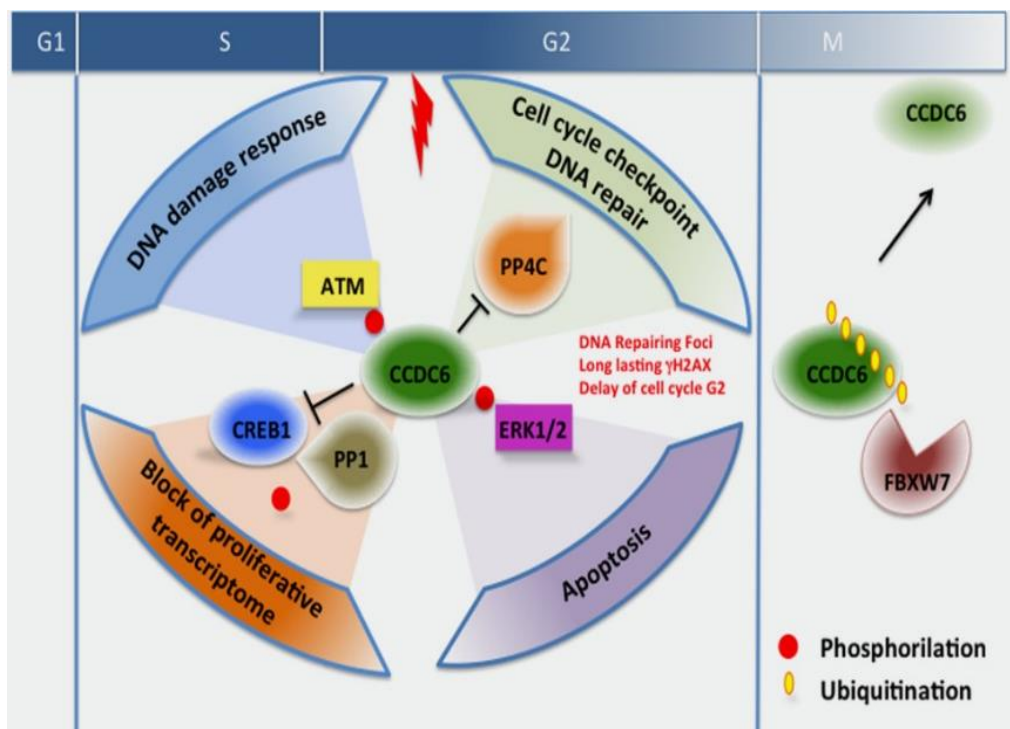


Figure 1.8 Summary of CCDC6 functions (Cerrato, Merolla, et al., 2018).

1.3.3 CCDC6 role as tumor suppressor gene in cancer

Due to its possible translocations, CCDC6 can lead to distinct types of cancer like leukemia, chronic myelomonocytic leukemia, breast, ovary and non-small lung cancer. These translocations lead to a change in the charge of CCDC6 protein which could promote cancer beside determining the homo-dimerization and transforming ability of the fusion oncoprotein (Cerrato, et al., 2018). According to these information, it was assumed that CCDC6 has an important role as a tumor suppressor gene and this purpose was proved in the experiment on CCDC6-ex2 knock-in mice as they developed thyroid hyperplasia an enhanced CREB1 activity and an increased expression of the CREB1 regulated genes (Leone et al., 2015). These evidences greatly approve an appropriate role for CCDC6 impairment in promoting tumor development. In addition, role of CCDC6 in causing cancer becomes obvious when it gets fused with different oncogenes, prominently with RET in thyroid cancer (**Figure 1.6**). Indeed, it was described that lung cancer patients who developed resistance to EGFR tyrosine kinase inhibitors have shown the presence of CCDC6-RET in post progression samples (Klempner et al., 2015). Finally, CCDC6 is not only a partner of different proteins but also it has been demonstrated that it could be mutated in distinct tumor types (**Figure 1.9 and Table 1**). The mutations can be either nonsense mutations that lead to dominant negative isoforms of CCDC6 or missense mutations that are believed to have each one of them a functional characterization but, still until nowadays, no systemic study was done to prove this purpose.

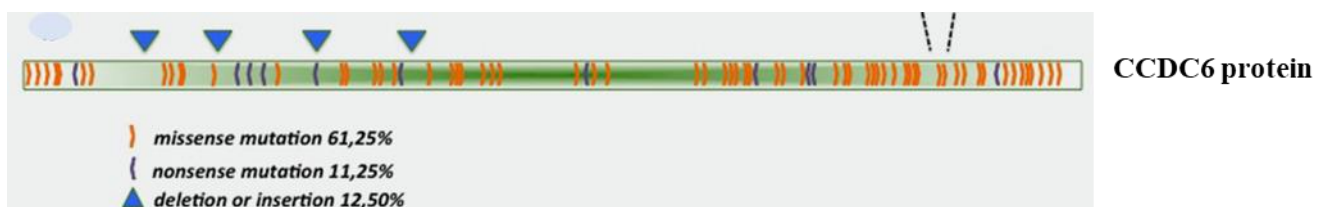


Figure 1.9 Mutations of CCDC6 protein found in cancer. CCDC6 protein diagram showing CCDC6 mutations identified in different cancer types: substitution nonsense (11.25%) are distributed mostly downstream of the minimal dominant-negative region (mndr) sequence. Substitution missense (61.25%) are distributed along all the protein sequence. Insertion in frame (2.50%), insertion frameshift (1.25%), deletion inframe (6.25%), deletion frameshift (2.50%), for a total of 12,25% of the cases occur mostly along the first 250 aa of the protein (Cerrato, Merolla, et al., 2018).

1.4 Therapeutic approaches of CCDC6 in cancer

CCDC6 is very important for the good development of the cells. First of all, Cells with deficiency of CCD6 behave as BRCA defective cells which lead to the resistance to chemotherapeutic agents and contribute to an increased sensitivity to small molecule inhibitor of PARP1/2 (Morra et al.,

2017). The inhibition of PARP enzymes leads impaired repair of single strand breaks and double strand breaks as the cell will be lack of homologous recombination repair or loss of repair genes (Cerrato et al., 2016). In addition, CCDC6 is involved it the response to olaparib, a drug used in ovarian and lung cancer therapy. To have an efficient response of olaparib, the level of CCDC6 should be low in the cell. This is accomplished by the activity E3 ubiquitin ligase Fbxw7 that targets CCDC6 proteasome degradation whereas deubiquitinase Usp7 stabilizes it (Mantha et al., 2014) (Laxmi et al., 2019). For this reason, P5091, which is an inhibitor of Usp7, is used to lower the level of CCDC6 and thus sensitize even lung cancer cells that present normal CCDC6 levels (**Figure 1.10**).

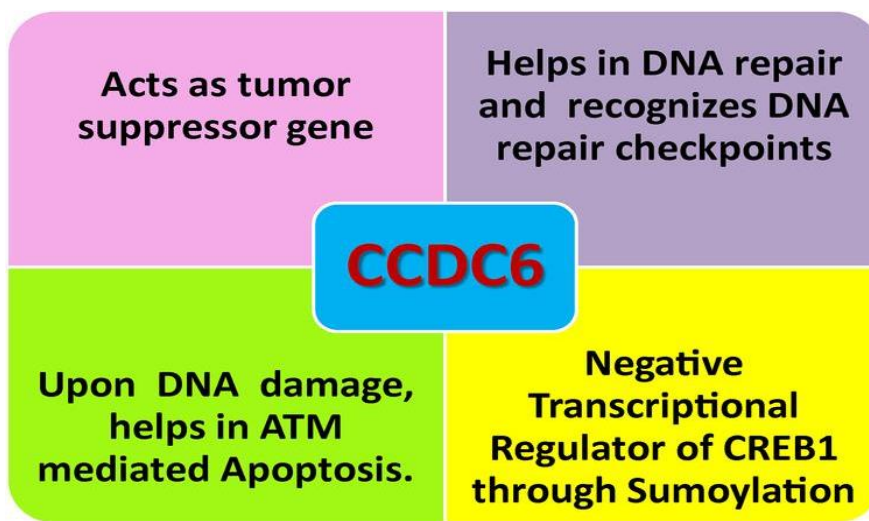


Figure 1.10 The various cellular modifiers of CCDC6 (Laxmi et al., 2019).

2 HYPOTHESIS AND OBJECTIVES

As it has been previously explained, MNT may play a key role in the proliferation of the tumor by interacting with distinct proteins and as it can be, at the same time, antagonist or cooperators of MYC. And, as our lab has discovered a new interaction of MNT and CCDC6 in Raji cells, so the general aim of this work is to gain further insight into the effect of MNT-CCDC6 interaction in CTCL-derived cell lines and the effect of MNT silencing on tumor proliferation. For this purpose, we established the following aims:

- Compare MNT and CCDC6 expression in several lymphoma B cell lines from our lab collection (Ramos, Raji, DG75) as well as in T cell lymphoma cells (Jurkat) and CTCL -derived cell lines (HuT78, Se-AX) and CTCL-mycosis fungoides (My-La).

- Investigate the MNT-CCDC6 interaction, in the cell lines with significant expression of both genes.

- Silence MNT in CTCL-derived cell lines by lentiviral infection and measure the proliferation.

3 MATERIALS AND METHODS

3.1 CELL CULTURE

In this work, many human cell lines, with different origins, were used. First, three types of Cutaneous T cell lymphoma (CTCL) cells were used not only for determining the expression of both genes MNT and CCDC6 but also for lentivirus infection experiments while silencing MNT and for Co-Immunoprecipitation experiments. These cells were MyLa derived from Mycosis Fungoides skin disease, SeAx and HuT 78 that are derived from peripheral blood and represent Sezary syndrome. Second, another line of T cell lymphoma (Jurkat) was used as control of MNT and CCDC6 expression. It is an immortalized T lymphocyte cell line that was originally obtained from the peripheral blood of a boy with T cell leukemia. Finally, some B cells also were used in this work which are the Burkitt lymphoma Ramos cell line derived from ascites, and DG75 cell line which is Burkitt lymphoma cell line derived from pleural effusion.

In addition, HeLa pLKO cells were used for transfection in order to prepare positive controls of MNT and CCDC6. These are HeLa cells transduced with the lentiviral pLKO empty vector, HeLa cells derive from cervical cancer. Lymphoma-derived were grown in basal media RPMI (Roswell Park Memorial Institute) medium for suspension cell culture, and HeLa cells in DMEM (Dulbecco's Modified Eagle Medium) for adherent cell culture; Gibco™) supplemented with 10% fetal bovine serum (FBS, Gibco™), 150 µg/ml gentamycin and 2 µg/ml ciprofloxacin. All cell lines were maintained at 37 °C in a humidified 5% CO₂ atmosphere.

3.2 EXTRACTION OF DNA

3.2.1 EXTRACTION OF DNA (MNT+CCD6)

For plasmid preparation, bacteria were grown overnight at 37°C with agitation in 250 ml of L Broth supplemented with 100 µg/ml ampicillin. The next day, the cell pellet was processed with a GeneJet plasmid MiniPrep kit (Thermo Scientific). After that, we added 3.5 ml of pure isopropanol, covered with parafilm and mixed by inversion then centrifuged at 10,000 rpm at JS13.1 / 30 min at 4°C. Thirty minutes after, we discarded carefully the supernatant. Finally, the DNA pellet was washed with 1 ml of 70% ethanol. The DNA pellet at the bottom are left to dry in a flow cabinet for 15 min, and then resuspended in 50-100 µl of water, depending on the size of DNA pellet and left it resuspending at 4°C overnight. The next day, we transferred it to an Eppendorf and quantify the concentration in the nanodrop.

3.2.2 PREPARATION OF POSITIVE CONTROLS

The first day, a HelapLKO cryotube was thawed in a p100 with 10 ml DMEM-10% FCS. The next day, the cells were passed 1:2 (7ml DMEM-10% FCS+5ml cell suspension). Three days after, as the cells are adherents, so the medium was aspirated and peeled off with trypsin then DMEM-10% FCS

was added up to 12 ml and the cells were counted: 1.93×10^6 cells/ml. The cells were putted in two P100 with 2×10^6 cells per plate (2 ml cell suppression+8 ml DMEM-10% FCS) and the rest of the cells were frozen (2 cryotubes with 9.5 million cells each). The next day, the plasmids needed that were at -20°C : CCDC6 (pcDNA CCDC6-MYC wt) which was the concentration $0.2625 \mu\text{g}/\mu\text{l}$ and MNT (pcDNA 3.1 MNT-HA wt (**Figure 3.2**)) with the concentration $0.4 \mu\text{g}/\text{ml}$, were thawed. After, $10 \mu\text{g}$ DNA from each plasmid ($38 \mu\text{l}$ CCDC6, $25 \mu\text{l}$ MNT) was collected in 2 Eppendorfs and added $250 \mu\text{l}$ NaCl 150 mM and I mixed, in a falcon, $40 \mu\text{l}$ PEI ($20 \mu\text{l}$ per Eppendorf) and $460 \mu\text{l}$ NaCl 150 mM ($230 \mu\text{l}$ per Eppendorf). After that, I mixed carefully $250 \mu\text{l}$ of plasmid with $250 \mu\text{l}$ of polyethylenimine (PEI)-NaCl mix, pouring PEI over DNA slowly along the wall and incubate the mix for 30 min at room temperature. Finally, I added the $500 \mu\text{l}$ of plasmid+PEI-NaCl to the cells, dropwise, on the HeLa pLKO of p100 and incubated them 36 h at 37°C . Two days after, I aspirated the medium, peeled off the cells with trypsin, added 4 ml DMEM-10% FCS, centrifuged at $1500 \text{ rpm}/3 \text{ min}$, washed with 1 ml PBS, and centrifuged again at $1500 \text{ rpm}/3 \text{ min}$ and the pellets were collected and putted in ice. After that, I added $200 \mu\text{l}$ of lysis buffer with IP and IF (no matter how many cells there are) per sample and incubated them for 15 min on ice. Then, the samples were sonicated (10 cycles, 30 s ON, 30 s OFF) and centrifuge at $14000 \text{ rpm}/20 \text{ min}$ at 4°C . Finally, I transferred the supernatant to clean tubes and froze them at -80°C until the next western blot. Experiment schematized in **Figure 3.1**.

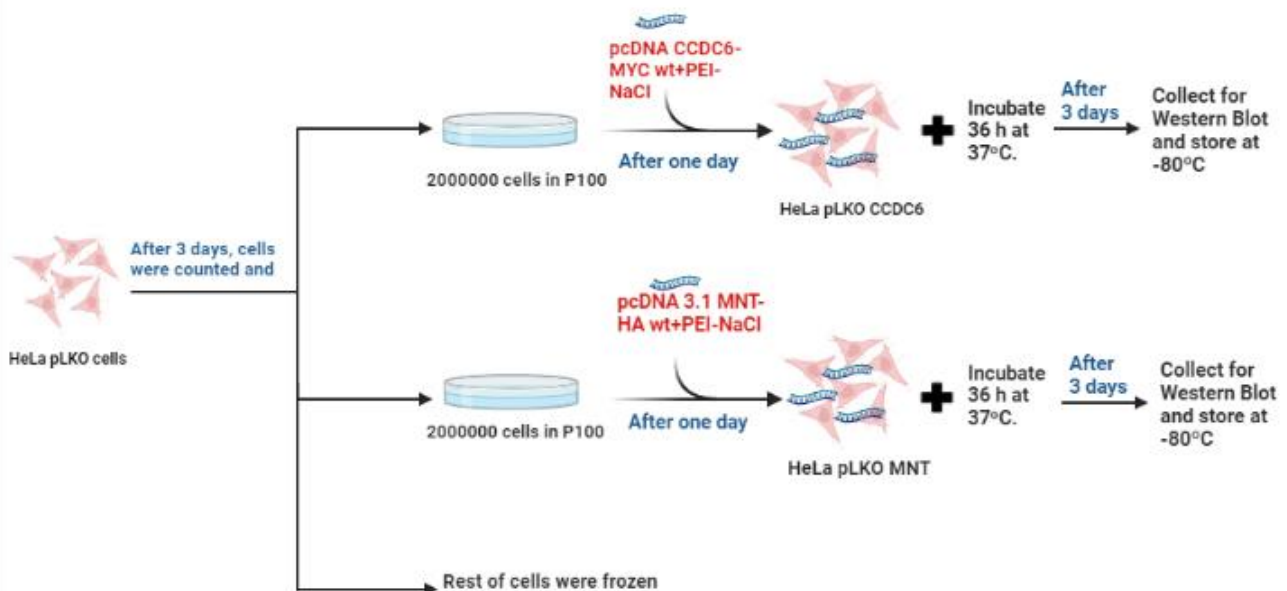


Figure 3.1 Preparation of positive controls experiment.



Figure 3.2 Scheme of the MNT expression vector used. This cDNA was cloned into the pcDNA 3.1 vector. SID for SIN3 Interaction Domain; bHLHLZ for basic-loop-helix leucine zipper domain; HA for hemagglutinin tag.

3.3 PROTEIN EXTRACTION AND QUANTIFICATION

3.3.1 CELL LYSIS, PROTEIN EXTRACTION AND QUANTIFICATION

Protein levels were analyzed by western blot. Distinct number of cells was collected by centrifugation, washed with TTBS and stored and -80 °C until protein extraction. The pellets were lysed with RIPA lysis buffer: 50 mM Tris-HCL, 150 mM NaCl, 1% Igepal, 0.5% deoxycholic acid and 0.1% Sodium dodecyl sulphate SDS. Per 5 million cells, a mix of 150 µl of RIPA and 1.5 µl of each inhibitor was prepared. The inhibitors were protease inhibitor cocktail Set I (1:100; Calbiochem) and phosphatase inhibitor cocktail I (1:100; Sigma-Aldrich®). After mixing the samples with the complex prepared, they were putted in ice for 15min, then sonicated at 4 °C with a mode of 10 cycles with 30 s on/off. Ten minutes after, the samples were centrifuged at 14000 rpm/20 min at 4°C. Finally, the supernatant was taken to a new Eppendorf and stored at -80 °C. Before storing them, the quantification of protein was done with mixing 1 µl of each sample with 199 µl of Qubit protein buffer and 1 µl of fluorophore and read in a Qubit fluorimeter.

3.3.2 WESTERN BLOT

The western blot is composed of three principal steps: Electrophoresis, Transfer of protein to membrane and Hybridization. Sodium dodecyl sulphate polyacrylamide gel electrophoresis (SDS-PAGE) is used to separate proteins according to their molecular weights.

Before starting the electrophoresis in 10% acrylamide gel, the samples were mixed with water and 5X Laemmli (100 mM Tris-HCl pH 6.8, 5% mercaptoethanol, 5% SDS, 50% glycerol, 0.1% bromophenol blue) for a final concentration 1X in 25 μ l as a final volume. All samples had the same amount of proteins in all of them (50 μ g per sample) and the volume was adjusted with water so all have an equal volume to be loaded in the gels. After that, the mixed samples were heated in 95°C for five minutes and charged in the SDS-PAGE gel. The electrophoresis was performed at a constant voltage of 180 V in the running buffer TGS (25 mM Tris, 192 mM glycine and 0.1% SDS). Usually, between one hour to one hour and a half was needed for the migration of the protein to the end of the gel.

Then, the proteins were transferred to a nitrocellulose membrane AmershamProtran Supported 0.45 NC (GE Healthcare Life Sciences), with 0.45 μ m pore size, in a Mini-Trans Blot cell (Bio-Rad) using transfer buffer TG-MeOH (25 mM Tris, 192 mM glycine, and 10% methanol). One hour was needed to have a good transfer as we assumed 1 min per kDa, for proteins smaller than 60 kDa, and the proteins that I was interested on have a molecular weight between 62 and 75 kDa. The transference was performed on ice to avoid the overheating.

One hour after, the transfer was stopped. The gel was stained with Coomassie Brilliant Blue solution (0.025% Coomassie Brilliant Blue R-250, 40% methanol and 10% acetic acid) for 10 min at RT with shaking and destained with water to check proteins load. The membrane was incubated with 1g of non-fat dry milk and 10ml TTBS (20 mM Tris-HCl pH 7.5, 150 mM NaCl and 0.05% Tween 20 in distilled-water) for one hour at room temperature in order to block non-specific binding of other proteins.

Finally, the membrane was washed several times with TTBS and incubated with its specific primary antibody (**Table 2**) overnight at 4°C and in agitation. The primary antibodies were diluted at 1:1000 in 1% BSA-TTBS.

Table 2. Primary antibodies used for Western Blot and Co-Immunoprecipitation

Primary antibody	Molecular weight (kDa)	Specie	Origin
Anti-MNT	72	Rabbit	Novus (NBP2-04052)
Anti-MNT	62	Rabbit	Bioworld (BS5798)
Anti-CCDC6	65	Mouse	Santa Cruz (SC-100309)
Anti-β-Actin	42	Mouse	Santa Cruz (SC-47778)
IgG	—	Rabbit	Cell signaling (2729S)

The next day, the membrane was washed with TTBS for 15 min three times then incubated, for 45 min in dark, with a fluorescent secondary antibody (**Table 3**), which was from the same specie as the first one, before being scanned with the Odyssey® software and the amount of protein was quantified with ImageJ and normalized to a constitutively expressed protein, such as actin. The secondary antibodies were diluted at 1:10000 in 1% BSA-TTBS. Experiment schematized in **Figure 3.3**.

Table 3. Secondary antibodies used for Western Blot

Secondary antibody	Type	Origin
Anti-Mouse IRDye®680	Donkey polyclonal	LI-COR (926-68072)
Anti-Mouse IRDye®800	Donkey polyclonal	LI-COR (926-32212)
Anti-Rabbit IRDye®680	Donkey polyclonal	LI-COR (926-68073)

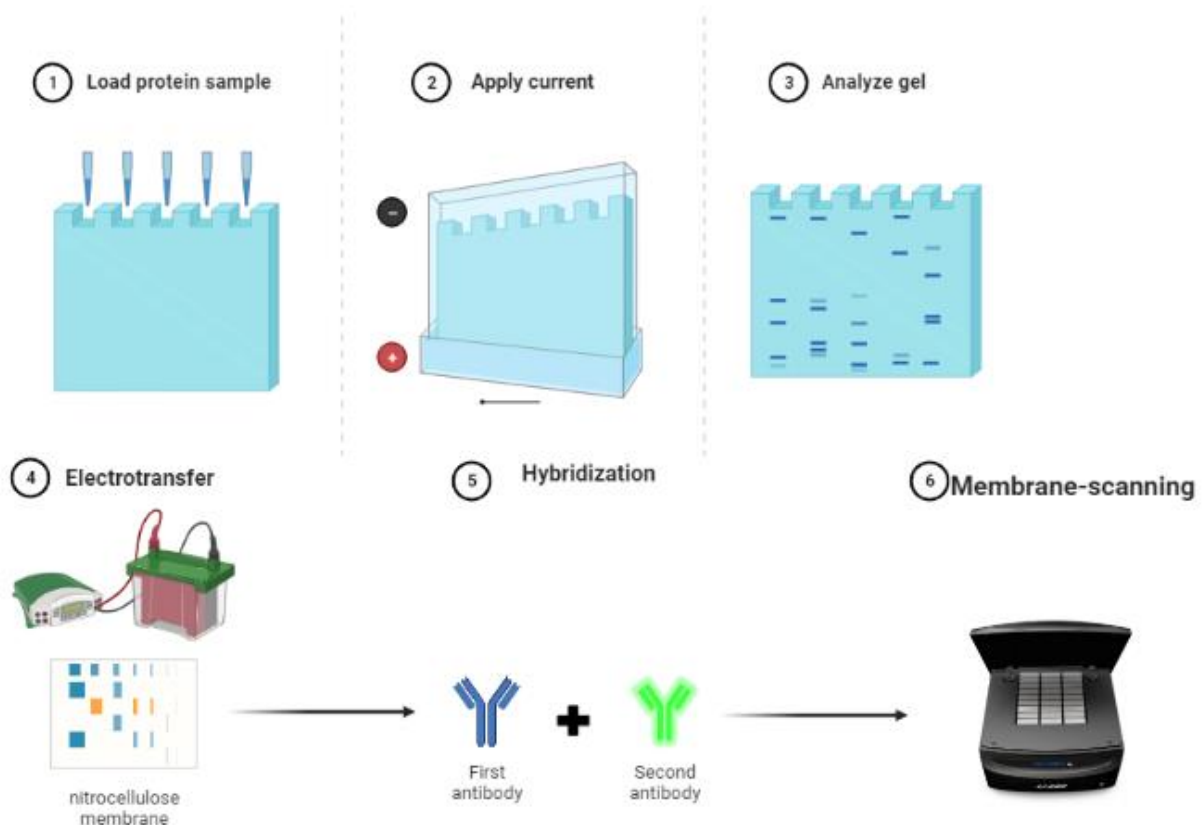


Figure 3.3 Scheme of the Western Blotting experiment.

3.4 CO-IMMUNOPRECIPITATION

3.4.1 PROTEIN LYSATES PREPARATION

Cells were lysed in 500 μ l of RIPA buffer containing the protease and phosphatase inhibitors cocktail. For co-immunoprecipitation experiment, the pellets weren't sonicated. Cell lysates were incubated rotating at 4 degrees in the wheel of cold room for 30 min. After incubation, cell lysates were centrifuged at 14000 rpm/20 min at 4°C. After that, the supernatant, that contains the proteins, was collected for protein immunoprecipitation. Proteins were quantified and 0.5 -1 mg of protein was used for each immunoprecipitation. Once the volume was calculated, 10 μ l of each sample is taken for the input and stored at -80 degrees. Then, each sample was divided: 1/2 of the volume was separated to be immunoprecipitated with IgG (**Table 2**) which was used as a control and 1/2 of the volume was immunoprecipitated with 3 μ l of anti-MNT (**Table 2**) and incubated in a wheel at 4°C overnight.

3.4.2 DYNABEADS IMMUNOPRECIPITATION

Proteins were immunoprecipitated with Dynabeads-protein G (00606149, Thermo Scientific) to capture protein-antibody complexes, were used. 15 μ l of Dynabeads were used per sample. The beads were first washed with washing buffer (2.5 ml Tris-HCl 1M, 1.5 ml NaCl 5M, 125 μ l IGEPAL, H₂O up to 50 ml). After the last wash, the Dynabeads were resuspended in double volume (30 μ l) of RIPA lysis buffer and mixed with 200 -1000 μ g of protein (also in RIPA buffer) and incubated in a wheel for 2 h at 4°C. After the incubation, the Dynabeads were separated with the magnet and the supernatant was collected as the negative control. Then, the immunocomplexes-beads were washed with 1 ml of cold washing buffer for 10 min 3 times, at 4°C. Once the washing was finished, the immunocomplexes-beads were resuspended in 30 μ l of Laemmli 2X to elute the proteins from the beads. Non-immunoprecipitated lysates (input) were also mixed with 5x Laemmli buffer to a 2X final concentration :10 μ l of input + 10 μ l Laemmli 5X. Finally, the samples were heated for 10 min at 95°C, then the magnetic beads were removed with the magnet and the supernatant was collected and runned in Western Blot or stored at -20°C. The technique is schematized in **Figure 3.4**.

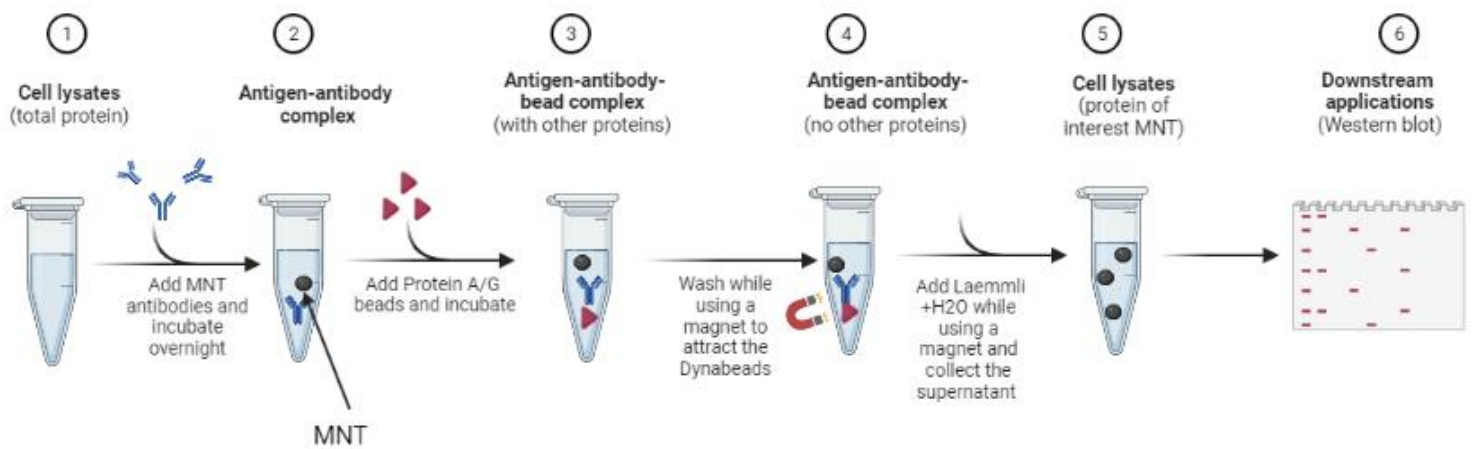


Figure 3.4 Scheme of the coimmunoprecipitation experiment.

3.5 LENTIVIRAL INFECTION AND PROLIFERATION ASSAY

The cells that were used for this experiment are CTCL-derived cell lines: MyLa, SeAx and HuT78. The cells were growing in 10 ml RPMI-10% FCS, with refreshing the medium after two days. After that, the cells were transferred to a P60 plate after being infected with two types of lentivirus: pLKO the empty lentivirus vector (**Figure 3.6**) and shMNT, encoding a short-hairpin construct for human MNT gene, in the presence of Polybrene (5 $\mu\text{g/ml}$) to enhance the efficiency of the lentiviral infection. After one day of the infection, puromycin (1 $\mu\text{g/ml}$) was added in order to select the infected cells and at the same time, the cells were passed to 96-well plate with a 2×10^4 cell/well and the remaining volume continued growing in P60. Three, and four days after, first of all, 10 μl of WST-1 reagent was added to the cells in T96 for two hours then the proliferation was measured in a plate colorimeter scanner (Multiskan FC). The WST-1 assay protocol is based on the cleavage of the tetrazolium salt WST-1 to formazan by cellular mitochondrial dehydrogenases. An aliquot of the lentiviral-infected cells, after three days, was collected as above and stored at -80°C to perform Western Blot as described above in order to check the silencing of MNT expression. Experiment schematized in **Figure 3.5**.

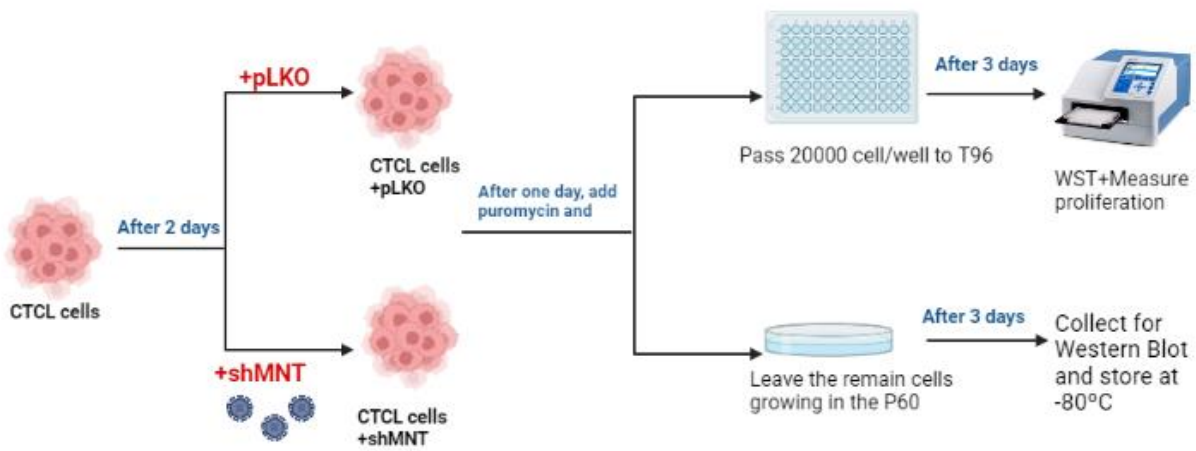


Figure 3.5 Scheme of the lentiviral infection and proliferation assay experiment.

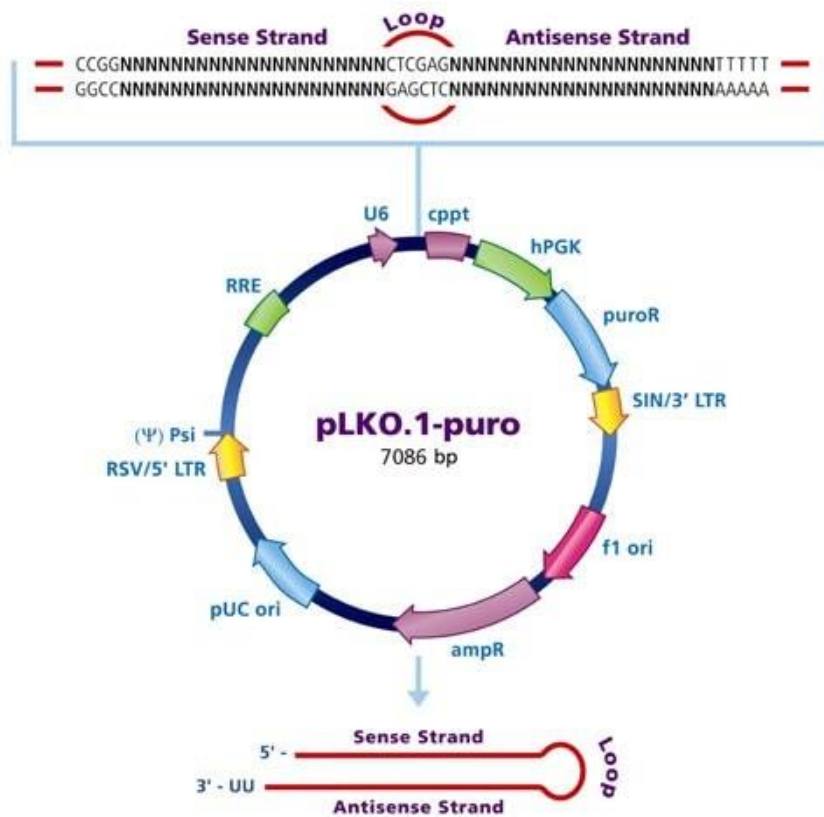


Figure 3.6 Maps of the vectors used in this work. pLKO.1-puro the empty lentivirus vector

4 RESULTS

4.1 MNT AND CCDC6 EXPRESSION

MNT plays, not only, a huge role in supervising the oncogenic activities of MYC, but also has a relevant role in cell biology as it is a fundamental protein for the development. For this reason, we decided to analyze the protein levels of MNT, with western blot, in different cell lines as it is evolutionarily conserved. For this experiment, we prepared a MNT positive control by transfecting HeLa pLKO with pcDNA 3.1 MNT-HA (0.4 μ g/ml) and a CCDC6 positive control by transfecting HeLa pLKO with pcDNA CCDC6-MYC wt (0.2625 μ g/ μ l), and the lysates were prepared as described in Materials and methods. We chose a few human cell lines from the B- and T-cell lineage (Ramos, DG75, MyLa, SeAx, Jurkat and HuT78) to study MNT functions in CTCL. The expression of MNT was detected in all the cell lysates used except Jurkat cells (**Figure 4.1**). MNT expression was more relevant in DG75 and HuT78 cells than the other cell lines.

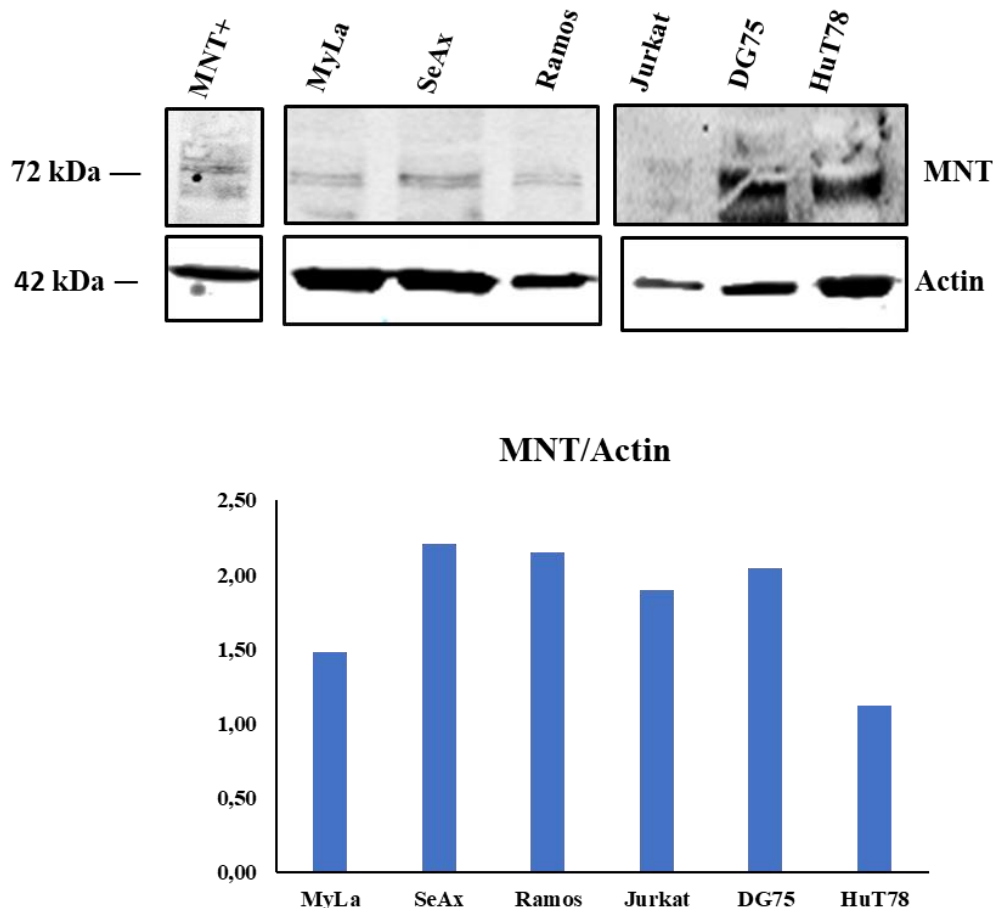


Figure 4.1 MNT expression in distinct cell lines. The protein level of MNT was analyzed by western blot, using the anti-MNT (Novus) which has a molecular weight of 72 kDa and β -actin, with a molecular weight of 42 kDa, used as a protein loading control. HeLa pLKO, overexpressing MNT, were used as a positive control for MNT. Lower panel: expression of MNT normalized to actin expression after densitometry of the blot shown in the upper panel.

Also, as the objective is to study MNT and CCDC6 interaction in CTCL-derived cell lines we decided first, to check the expression of CCDC6 in the same B- and T-cell lineage cell lines used before. CCDC6 protein was detected in all the cell lysates (**Figure 4.2**). The expression was similar in all the cell lines.

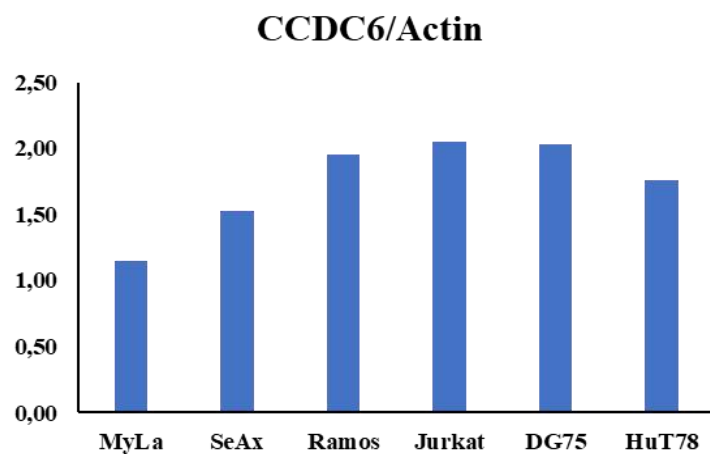
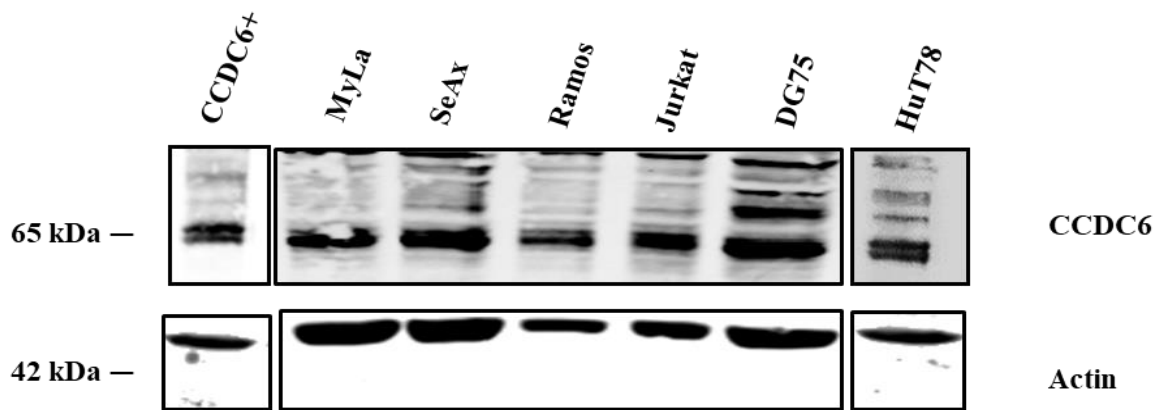


Figure 4.2 CCDC6 expression in distinct cell lines. The protein level of CCDC6 was analyzed by western blot, using the anti-CCDC6 which has a molecular weight of 65 kDa and β -actin, with a molecular weight of 42 kDa, used as a protein loading control. HeLa pLKO, overexpressing CCDC6, were used as a positive control for CCDC6. Lower panel: expression of CCDC6 normalized to actin expression after densitometry of the blot shown in the upper panel.

4.2 MNT-CCDC6 interaction

After having a good expression of MNT and CCDC6 in CTCL-derived cell lines: MyLa, SeAx and HuT78, we decided to check if there is any interaction between MNT and CCD6 in these cell lines by co-immunoprecipitation followed by a western blot. The results suggest that there is not an interaction between MNT ad CCDC6. However, the results must be confirmed with a positive control for interaction

of MNT as MAX. Unfortunately, the antibodies against MAX did not work and new antibodies were not available when this Master Thesis was submitted (**Figure 4.3**).

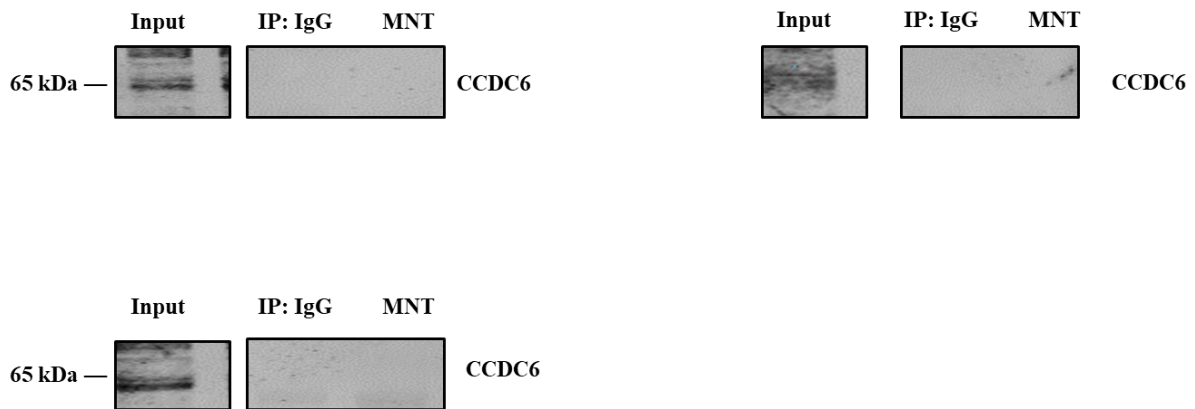


Figure 4.3 MNT and CCDC6 interaction in several cell lines. Co-immunoprecipitation assays in human cell lines by immunoprecipitating with anti-MNT (Novus) and hybridization with anti-CCDC6 (Q23).

4.3 EFFECT OF MNT DEPLETION ON CTCL CELL PROLIFERATION

To study MNT involvement in CTCL-derived cell lines proliferation, we decided to silence it using short hairpin (sh) technology. MyLa, SeAx and HuT78 were infected with the lentiviral particles pLKO (empty vector) and shMNT (pLKO expressing short hairpins for human MNT). After infection, cells were selected with puromycin for three and four days (**Figure 3.5**). The proliferation was measured after adding WST (**Figure 4.4b**) and the process of silencing MNT was proved by western blot (**Figure 4.4a**), using anti-MNT (**Table 2**). Silencing MNT was successful in two of the cell lines tested: MyLa and SeAx (**Figure 4.4a**) and this silencing was accompanied by an increase of proliferation (**Figure 4.4b**).

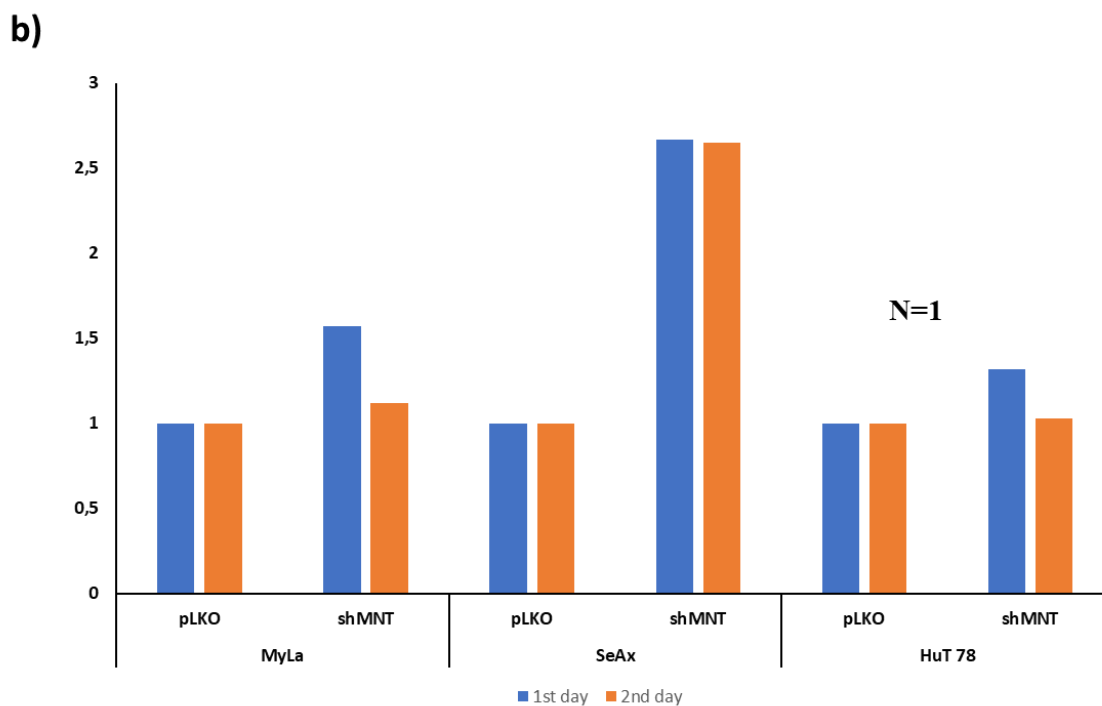
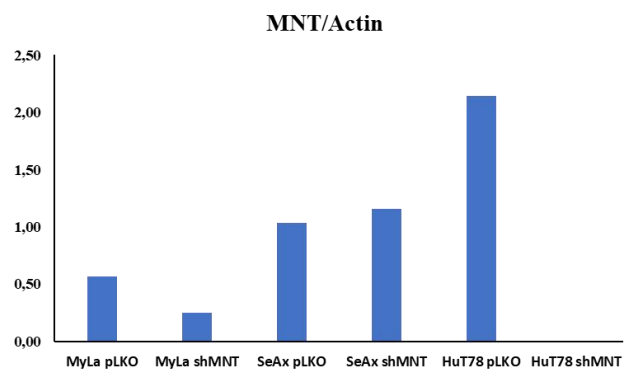
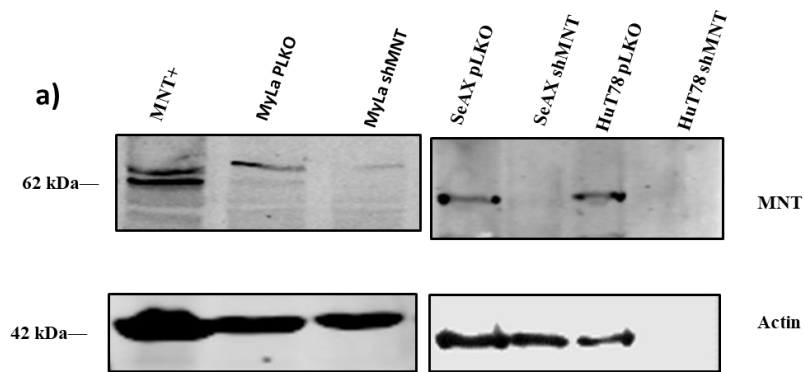


Figure 4.4 Assessment of silencing MNT in CTCL-derived cell lines. a) Western blot for checking that the silencing was successful while using anti-MNT. Lower panel: expression of MNT normalized to actin expression after densitometry of the blot shown in the upper panel. b) Measure of the proliferation for two different days: 1st day was after 3 days with puromycin and 2nd day was after 4 days with puromycin.

5 DISCUSSION

MNT has been described as an important regulator of MYC oncoprotein. Depending on the cell type and model under study, MNT behaves either as a MYC cooperator or MYC antagonist, as described in the Introduction. As MYC have been revealed so far as an undruggable oncoprotein, the research focus is being displaced to other proteins of the MYC network. From these MNT is the most relevant as it is ubiquitously expressed and because MNT deregulation and LOH (loss of heterozygosity) is found in cancer.

MNT is the most ubiquitously protein of the MXD family and controls several cellular functions as DNA damage, apoptosis and proliferation. MNT is activated in most human cancers which was also proved with the work of this Thesis as the expression of MNT was relevant in all the cell lines used except Jurkat cells (**Figure 4.1**). But, a work from our laboratory, has demonstrated that MNT is expressed at high levels in Jurkat cells (Liaño pons et al., 2021), so we can conclude that MNT is expressed in the different cell lines used, in the B-cell lineage: Ramos and DG75; and in the T-cell lineage: MyLa, SeAx, Jurkat, and HuT78. In this work we have focused on the MNT-CCDC6 interaction originally discovered in my Master thesis group at IBBTEC.

CCDC6 is an important protein in cell biology as it has a relevant role in the process of the repair of DNA double strand breaks DSB and for the cell mitotic entry (Cerrato et al., 2019). Also, CCDC6 is a tumor suppressor that mediates apoptosis in lymphoma cells. CCDC6, like MNT, is expressed in most human tissues and in many tumors. However its expression in cells derived from CTCL has not been asked, we have shown in this Master Thesis that CCDC6 was expressed in all the cell lines including MyLa,SeAx and HuT78 which are derived from human CTCL (**Figure 4.2**).

As our laboratory had discovered an interaction between MNT and CCDC6 in UR61 cells (rat cells), we tried to prove that this interaction could be also possible in cancer human cells. However, we could not detect MNT-CCDC6 interaction in the CTCL cell lines used for this project (**Figure 4.3**). This lack of interaction could be related to the role that MNT downregulation in CTCL. It is conceivably that the interaction with CCDC6 is required for MNT to limit proliferation, acting as an MNT negative regulator. However, in CTCL this antiproliferative interaction is abolished leading to higher proliferation of CTCL cells expressing MNT.

Finally, as it was mentioned in the introduction, MNT has an important role in the tumor proliferation, but no data were available in CTCL cells, despite that loss of heterogeneity of MNT is a common finding in CTCL. We have analyzed the effect of MNT ablation (mediated through siRNA technology) on CTCL cell proliferation and we found that si-RNA-mediated MNT silencing resulted in a higher proliferation rate in two of the cell lines tested. Our results are consistent with those previously reported showing that *Mnt*-deficient MEFs proliferated faster and the level of *Myc* decreased (reviewed

in Liaño pons et al., 2021). Our results are consistent with the hypothesis that MNT in CTCL cells can cooperate with MYC rather than being a MYC antagonist.

6 CONCLUSION

1. MNT and CCDC6 are expressed in the human cancer cells MyLa, SeAx, Ramos, Jurkat, DG75 and HuT78, with distinct levels of expression.

2. MNT and CCDC6 don't interact in CTCL-derived cell lines: MyLa, SeAx, and HuT78, as assessed by coimmunoprecipitation.

3. Silencing MNT induces an increase of the proliferation in CTCL-derived cell lines.

7 FUTURE WORK

In order to confirm:

-The non-existence of the interaction between MNT and CCDC6 in CTCL cells, the coimmunoprecipitation should be repeated with adding the positive control MAX.

- That silencing MNT in CTCL increases the proliferation, the experiment should be repeated for at least two times with the same conditions and compare the results with the ones that are exist in this Thesis.

8 REFERENCES

- Ayer, D. E., Lawrence, Q. A., & Eisenman, R. N. (1995). Mad-Max transcriptional repression is mediated by ternary complex formation with mammalian homologs of yeast repressor Sin3. *Cell*, 80(5), 767-776.
- Campbell, K. J., Vandenberg, C. J., Anstee, N. S., Hurlin, P. J., & Cory, S. (2017). Mnt modulates Myc-driven lymphomagenesis. *Cell Death & Differentiation*, 24(12), 2117-2126.
- Carroll, P. A., Freie, B. W., Mathsyaraja, H., & Eisenman, R. N. (2018). The MYC transcription factor network: Balancing metabolism, proliferation and oncogenesis. *Frontiers of Medicine*, 12(4), 412-425.
- Cerrato, A., Merolla, F., Morra, F., & Celetti, A. (2018). CCDC6: The identity of a protein known to be partner in fusion. *International Journal of Cancer*, 142(7), 1300-1308.
- Cerrato, A., Morra, F., & Celetti, A. (2016). Use of poly ADP-ribose polymerase [PARP] inhibitors in cancer cells bearing DDR defects: The rationale for their inclusion in the clinic. *Journal of Experimental & Clinical Cancer Research: CR*, 35(1), 179.
- Cerrato, A., Visconti, R., & Celetti, A. (2018). The rationale for druggability of CCDC6-tyrosine kinase fusions in lung cancer. *Molecular Cancer*, 17(1), 46.
- Cowling, V. H., & Cole, M. D. (2006). Mechanism of transcriptional activation by the Myc oncoproteins. *Seminars in Cancer Biology*, 16(4), 242-252.
- Crouch, D. H., Fisher, F., Clark, W., Jayaraman, P. S., Goding, C. R., & Gillespie, D. A. (1993). Gene-regulatory properties of Myc helix-loop-helix/leucine zipper mutants: Max-dependent DNA binding and transcriptional activation in yeast correlates with transforming capacity. *Oncogene*, 8(7), 1849-1855.
- Delgado, M. D., & León, J. (2010). Myc roles in hematopoiesis and leukemia. *Genes & Cancer*, 1(6), 605-616.
- Dezfouli, S., Bakke, A., Huang, J., Wynshaw-Boris, A., & Hurlin, P. J. (2006). Inflammatory disease and lymphomagenesis caused by deletion of the Myc antagonist Mnt in T cells. *Molecular and Cellular Biology*, 26(6), 2080-2092.
- Gabay, M., Li, Y., & Felsher, D. W. (2014). MYC activation is a hallmark of cancer initiation and maintenance. *Cold Spring Harbor Perspectives in Medicine*, 4(6), a014241.
- Garcia-Sanz, P., Quintanilla, A., Lafita, M. C., Moreno-Bueno, G., García-Gutierrez, L., Tabor, V., Varela, I., Shii, Y., Larsson, L.-G., Portillo, F., & Leon, J. (2014). Sin3b Interacts with Myc and Decreases Myc Levels. *The Journal of Biological Chemistry*, 289(32), 22221-22236.
- Gartel, A. L., & Shchors, K. (2003). Mechanisms of c-myc-mediated transcriptional repression of growth arrest genes. *Experimental Cell Research*, 283(1), 17-21.

-Grieco, M., Santoro, M., Berlingieri, M. T., Melillo, R. M., Donghi, R., Bongarzone, I., Pierotti, M. A., Della Porta, G., Fusco, A., & Vecchio, G. (1990). PTC is a novel rearranged form of the ret proto-oncogene and is frequently detected in vivo in human thyroid papillary carcinomas. *Cell*, 60(4), 557-563.

-Grzenda, A., Lomberk, G., Zhang, J.-S., & Urrutia, R. (2009). Sin3 : Master scaffold and transcriptional corepressor. *Biochimica Et Biophysica Acta*, 1789(6-8), 443-450.

-Hurlin, P. J., Quéva, C., & Eisenman, R. N. (1997). Mnt, a novel Max-interacting protein is coexpressed with Myc in proliferating cells and mediates repression at Myc binding sites. *Genes & Development*, 11(1), 44-58.

-Hurlin, P. J., Zhou, Z.-Q., Toyo-oka, K., Ota, S., Walker, W. L., Hirotsune, S., & Wynshaw-Boris, A. (2003). Deletion of Mnt leads to disrupted cell cycle control and tumorigenesis. *The EMBO Journal*, 22(18), 4584-4596.

-Jiang, S. M. (2000). The RET proto-oncogene in human cancers. *Oncogene*, 19(49), 5590-5597.

-Kalkat, M., De Melo, J., Hickman, K. A., Lourenco, C., Redel, C., Resetca, D., Tamachi, A., Tu, W. B., & Penn, L. Z. (2017). MYC Deregulation in Primary Human Cancers. *Genes*, 8(6), 151.

-Kapoor, I., Kanaujiya, J., Kumar, Y., Thota, J. R., Bhatt, M. L. B., Chattopadhyay, N., Sanyal, S., & Trivedi, A. K. (2016). Proteomic discovery of MNT as a novel interacting partner of E3 ubiquitin ligase E6AP and a key mediator of myeloid differentiation. *Oncotarget*, 7(7), 7640-7656.

-Kay, B. K., Williamson, M. P., & Sudol, M. (2000). The importance of being proline: The interaction of proline-rich motifs in signaling proteins with their cognate domains. *FASEB Journal: Official Publication of the Federation of American Societies for Experimental Biology*, 14(2), 231-241.

-Klempner, S. J., Bazhenova, L. A., Braiteh, F. S., Nikolinakos, P. G., Gowen, K., Cervantes, C. M., Chmielecki, J., Greenbowe, J. R., Ross, J. S., Stephens, P. J., Miller, V. A., Ali, S. M., & Ou, S.-H. I. (2015). Emergence of RET rearrangement co-existing with activated EGFR mutation in EGFR- mutated NSCLC patients who had progressed on first- or second-generation EGFR TKI. *Lung Cancer (Amsterdam, Netherlands)*, 89(3), 357-359.

-Laxmi, A., Gupta, P., & Gupta, J. (2019). CCDC6, a gene product in fusion with different protooncogenes, as a potential chemotherapeutic target. *Cancer Biomarkers: Section A of Disease Markers*, 24(4), 383-393.

-Lee, T., Yao, G., Nevins, J., & You, L. (2008). Sensing and Integration of Erk and PI3K Signals by Myc. *PLoS Computational Biology*, 4(2), e1000013.

-Leone, V., Langella, C., Esposito, F., Arra, C., Palma, G., Rea, D., Paciello, O., Merolla, F., De Biase, D., Papparella, S., Celetti, A., & Fusco, A. (2015). Ccdc6 knock-in mice develop thyroid hyperplasia associated to an enhanced CREB1 activity. *Oncotarget*, 6(17), 15628-15638.

-Leone, V., Mansueto, G., Pierantoni, G. M., Tornincasa, M., Merolla, F., Cerrato, A., Santoro, M., Grieco, M., Scaloni, A., Celetti, A., & Fusco, A. (2010). CCDC6 represses CREB1 activity by recruiting histone deacetylase 1 and protein phosphatase 1. *Oncogene*, 29(30), 4341-4351.

-Liaño-Pons, J., Arsenian-Henriksson, M., & León, J. (2021). The Multiple Faces of MNT and Its Role as a MYC Modulator. *Cancers*, 13(18), 4682.

-Link, J. M., & Hurlin, P. J. (2015). The activities of MYC, MNT and the MAX-interactome in lymphocyte proliferation and oncogenesis. *Biochimica et Biophysica Acta (BBA) - Gene Regulatory Mechanisms*, 1849(5), 554-562.

-Link, J. M., Ota, S., Zhou, Z.-Q., Daniel, C. J., Sears, R. C., & Hurlin, P. J. (2012). A critical role for Mnt in Myc-driven T-cell proliferation and oncogenesis. *Proceedings of the National Academy of Sciences of the United States of America*, 109(48), 19685-19690.

-Loo, L. W. M., Secombe, J., Little, J. T., Carlos, L.-S., Yost, C., Cheng, P.-F., Flynn, E. M., Edgar, B. A., & Eisenman, R. N. (2005). The transcriptional repressor dMnt is a regulator of growth in *Drosophila melanogaster*. *Molecular and Cellular Biology*, 25(16), 7078-7091.

-Mantha, K., Laufer, B. I., & Singh, S. M. (2014). Molecular changes during neurodevelopment following second-trimester binge ethanol exposure in a mouse model of fetal alcohol spectrum disorder: From immediate effects to long-term adaptation. *Developmental Neuroscience*, 36(1), 29-43.

-Meroni, G., Reymond, A., Alcalay, M., Borsani, G., Tanigami, A., Tonlorenzi, R., Lo Nigro, C., Messali, S., Zollo, M., Ledbetter, D. H., Brent, R., Ballabio, A., & Carrozzo, R. (1997). Rox, a novel bHLHZip protein expressed in quiescent cells that heterodimerizes with Max, binds a non-canonical E box and acts as a transcriptional repressor. *The EMBO Journal*, 16(10), 2892-2906.

-Morra, F., Merolla, F., Napolitano, V., Ilardi, G., Miro, C., Paladino, S., Staibano, S., Cerrato, A., & Celetti, A. (2017). The combined effect of USP7 inhibitors and PARP inhibitors in hormone-sensitive and castration-resistant prostate cancer cells. *Oncotarget*, 8(19), 31815-31829.

-Orian, A., van Steensel, B., Delrow, J., Bussemaker, H. J., Li, L., Sawado, T., Williams, E., Loo, L. W. M., Cowley, S. M., Yost, C., Pierce, S., Edgar, B. A., Parkhurst, S. M., & Eisenman, R. N. (2003). Genomic binding by the *Drosophila* Myc, Max, Mad/Mnt transcription factor network. *Genes & Development*, 17(9), 1101-1114.

-Poole, C. J., & van Riggelen, J. (2017). MYC-Master Regulator of the Cancer Epigenome and Transcriptome. *Genes*, 8(5), E142.

-Rahl, P. B., & Young, R. A. (2014). MYC and Transcription Elongation. *Cold Spring Harbor Perspectives in Medicine*, 4(1), a020990-a020990.

-Rosenthal, A., & Younes, A. (2017). High grade B-cell lymphoma with rearrangements of MYC and BCL2 and/or BCL6: Double hit and triple hit lymphomas and double expressing lymphoma. *BloodReviews*, 31(2), 37-42.

-Schaub, F. X., Dhankani, V., Berger, A. C., Trivedi, M., Richardson, A. B., Shaw, R., Zhao, W., Zhang, X., Ventura, A., Liu, Y., Ayer, D. E., Hurlin, P. J., Cherniack, A. D., Eisenman, R. N., Bernard, B., Grandori, C., & Cancer Genome Atlas Network. (2018). Pan-cancer Alterations of the MYC Oncogene and Its Proximal Network across the Cancer Genome Atlas. *Cell Systems*, 6(3), 282-300.e2.

-Toyo-oka, K., Bowen, T. J., Hirotsune, S., Li, Z., Jain, S., Ota, S., Escoubet-Lozach, L., Lozach, L. E., Garcia-Bassets, I., Bassett, I. G., Lozach, J., Rosenfeld, M. G., Glass, C. K., Eisenman, R., Ren, B., Hurlin, P., & Wynshaw-Boris, A. (2006). Mnt-deficient mammary glands exhibit impaired involution and tumors with characteristics of myc overexpression. *Cancer Research*, 66(11), 5565-5573.

-Toyo-oka, K., Hirotsune, S., Gambello, M. J., Zhou, Z.-Q., Olson, L., Rosenfeld, M. G., Eisenman, R., Hurlin, P., & Wynshaw-Boris, A. (2004). Loss of the Max-interacting protein Mnt in mice results in decreased viability, defective embryonic growth and craniofacial defects: Relevance to Miller-Dieker syndrome. *Human Molecular Genetics*, 13(10), 1057-1067.

-Wahlström, T., & Henriksson, M. (2007). Mnt takes control as key regulator of the myc/max/mxd network. *Advances in Cancer Research*, 97, 61-80.

-Walker, W., Zhou, Z.-Q., Ota, S., Wynshaw-Boris, A., & Hurlin, P. J. (2005). Mnt-Max to Myc-Max complex switching regulates cell cycle entry. *The Journal of Cell Biology*, 169(3), 405-413.

-Xia, Y., & Zhang, X. (2020). The Spectrum of MYC Alterations in Diffuse Large B-Cell Lymphoma. *Acta Haematologica*, 143(6), 520-528.

-Zervos, A. S., Gyuris, J., & Brent, R. (1993). Mxi1, a protein that specifically interacts with Max to bind Myc-Max recognition sites. *Cell*, 72(2), 223-232.